JPET #90068

Measurement of the proportion of D$_2$ receptors configured in state of high affinity for agonists in vivo: a Positron Emission Tomography study using [11C]N-propyl-norapomorphine and [11C]raclopride in baboons.

Rajesh Narendran, Dah-Ren Hwang, Mark Slifstein, Yuying Hwang, Yiyun Huang, Jesper Ekelund, Olivier Guillin, Erica Scher, Diana Martinez, Marc Laruelle.

From the Departments of Psychiatry (R.N., D-R.H., M.S., Y.H., Y.H., J.E., O.G., E.S., D.M., M.L.) and Radiology (D-R.H., M.L.), Columbia University College of Physicians and Surgeons and the New York State Psychiatric Institute, New York, NY 10032

Running Title: PET Imaging of D₂ high affinity receptor density.

Address correspondence to:

R. Narendran, MD

New York State Psychiatric Institute

1051 Riverside Drive, Box #31

New York, NY 10032

Telephone: (212) 543-5731

Fax: (212) 568-6171

E-mail: rn2012@columbia.edu

Number of Text Pages: 42

 Number of Tables: 6

Number of Figures: 5

Number of References: 39

Number of Words in Abstract: 243

Number of Words in Introduction: 745

Number of Words in Discussion: 1500

Section Assignment: Neuropharmacology

List of Non standard Abreviations used:

     CA - carrier added conditions (pharmacological doses)

     NCA - non- carrier added conditions (tracer doses)

     BCI - bolus plus constant infusion paradigm

     BBB - blood-brain barrier

K_{bol} - the time that would be required to inject the bolus at the infusion rate in minutes

ROI - regions of interest

AIR - automated image registration

(+)-PD 128907 - (S)-(+)-(4aR,10bR)-3,4,4a,10b-Tetrahydro-4-propyl-2H,5H-[1]benzopyrano-[4,3-b]-1,4-oxazin-9-ol hydrochloride

ABSTRACT

Dopamine D_2 receptors are configured in interconvertible states of high ($D_{2\ high}$) or low ($D_{2\ low}$) affinity for agonists. The in vivo proportion of sites in high affinity state remains poorly documented. Previous studies have established the D2 agonist [^{11}C] N-propyl-norapomorphine (NPA) as a suitable Positron Emission Tomography radiotracer for imaging $D_{2\ high}$ in the living brain. To elucidate the proportion of D_2 receptors configured in $D_{2\ high}$ states in vivo, imaging studies were conducted in three baboons with both [^{11}C]NPA and the D_2 receptor antagonist [^{11}C]raclopride. These studies were performed under non carrier added and carrier added conditions, to compare the B_{max} of [^{11}C]NPA and [^{11}C]raclopride in the same animals. [^{11}C]RAC in vivo K_D and B_{max} were 1.59 ± 0.28 nM (n = 3) and 27.3 ± 3.9 nM (n = 3), respectively. The in vivo K_D of [^{11}C]NPA was 0.16 ± 0.01 nM (n = 3), consistent with its affinity for $D_{2\ high}$ reported in vitro. The maximal density of sites for [^{11}C]NPA was 21.6 ± 2.8 nM (n = 3), i.e 79% of the [^{11}C]raclopride B_{max}. This result suggested that 79% of D_2 receptors are configured as $D_{2\ high}$ in vivo. This large proportion of $D_{2\ high}$ sites might explain the vulnerability of D_2 radiotracers to competition by endogenous dopamine, and is consistent with a previous report that the in vivo binding of agonist radiotracer [^{11}C]NPA is more vulnerable to competition by endogenous dopamine than that of antagonist radiotracer [^{11}C]raclopride.

INTRODUCTION

The dopamine system plays an important role in the modulation of a large number of neuronal functions, including movement, drive and reward, and alterations of dopamine transmissions are involved in numerous neuropsychiatric conditions, such as Parkinson's disease, schizophrenia and substance abuse. Dopamine receptors belong to two families of receptors, D_1-like (including D_1 and D_5 receptors) and D_2-like (including D_2, D_3 and D_4) receptors (Seeman and Van Tol, 1994). Like all G-protein linked receptors, the affinity of D_2-like receptors for agonists is affected by the coupling of the receptors with G proteins. The high affinity sites (D_{2high}) are G protein-coupled, while the low affinity sites (D_{2low}) are those uncoupled with G protein. In vitro homogenate binding studies suggest that approximately 50% of D_2 receptors are configured in the D_{2high} state (Sibley et al., 1982). However, very little is known about the proportion of D_2 receptors that are configured in $D_{2\ high}$ state (%R_{high}) in vivo.

Over the years, antagonists and inverse agonists such as [^{11}C]raclopride and [^{11}C]N-methyl-spiperone have been developed as radiotracers for imaging D_2-like receptors using positron emission tomography (PET). As these antagonists and inverse agonists binds with equal affinity to both $D_{2\ high}$ and $D_{2\ low}$ receptors, or tends to preferentially bind to the $D_{2\ low}$, they cannot provide information about the $D_{2\ high}$ receptors (Roberts and Strange, 2005).

(-)-N-Propyl-norapomorphine (NPA) is a full agonist at the D_2 and D_3 receptors (Neumeyer et al., 1973; Gardner and Strange, 1998). The in vitro affinity of NPA for D_{2high} and D_{2low} sites have been reported to be in the range of 0.07 to 0.4 nM and 20 to 200 nM respectively, suggesting a 50 to 200 fold selectivity for D_{2high} compared to $D_{2\ low}$ sites (for references see Table 1).

Hwang et al. (2000) reported a procedure to radiolabel NPA with C-11, as well as initial imaging experiments in baboons using [11C]NPA. In baboons, [11C]NPA demonstrated a rapid brain uptake with selective accumulation in the striatum. The striatal uptake was decreased to the level of cerebellar uptake following pretreatment with the D_2 receptor antagonist haloperidol, indicating that the striatal uptake of [11C]NPA was saturable and selective for D_2-like receptors. Furthermore, the uptake kinetics of [11C]NPA were fast and amenable to quantitative analysis. In baboons, the binding potential (BP) of [11C]NPA in the striatum was reported as 4.04 ± 1.05 mL g^{-1} (Hwang et al., 2004).

Under tracer conditions, the BP of a radiotracer is proportional to the product of the site density (B_{max}) and affinity ($1/K_D$),

$$BP = f_1 \frac{B_{max}}{K_D} \qquad \text{Eq. 1}$$

where f_1 is the free fraction of the ligand in plasma. [11C]NPA BP is the sum of the BP for $D_{2\,high}$ (BP_{high}) and $D_{2\,low}$ (BP_{low}). Denoting by R_{high} and R_{low} the densities of high and low affinity sites, and $1/K_{high}$ and $1/K_{low}$ the affinities of [11C]NPA for high and low affinity states, [11C]NPA BP (BP_{NPA}) can be expressed as

$$BP_{NPA} = BP_{High} + BP_{Low} = f_1 \left(\frac{R_{high}}{K_{high}} + \frac{R_{low}}{K_{low}} \right) \qquad \text{Eq. 2}$$

from which it appears that the contribution of BP_{low} to BP_{NPA} is likely to be small. For example, if we assume based on in vitro homogenate binding studies that in vivo 20-50% of the sites are configured in R_{high} and use the values reported by (Gardner and Strange, 1998) in Table 1 for K_{high} and K_{low}, the contribution of BP_{low} to BP_{NPA} would be approximately 9.6-2.3%.

Further characterization of BP_{NPA} requires in vivo measurement of K_{high}, K_{low}, R_{high} and R_{low}. As it was anticipated that the low affinity of [11C]NPA for $D_{2\,low}$ would preclude the detection of the in vivo binding of [11C]NPA to $D_{2\,low}$, this question was approached by

measuring [^{11}C]NPA K_{high} and R_{high}, and calculating %R_{high} by comparing R_{high} to the B_{max} of

the antagonist [^{11}C]raclopride measured in vivo in the same animals.

Thus, in the present study, PET experiments were conducted in three baboons under non-

carrier added (NCA) conditions (tracer doses) and under carrier added (CA) conditions

(pharmacological doses) to estimate the in vivo affinity and maximal density of binding sites of

[^{11}C]NPA and [^{11}C]raclopride. Experiments were conducted using the bolus plus constant

infusion paradigm, which produces a state of sustained binding equilibrium at the level of the

receptors (Laruelle et al., 1994a; Laruelle et al., 1994b). Data were analyzed using three

methods: simple equilibrium analysis (based on the analysis of the data during the equilibrium

interval), kinetic analysis (based on the arterial input function), and a mixed method, denoted

modeled equilibrium analysis, with peak equilibrium values estimated from the kinetic fit of the

data (Slifstein et al., 2004b).

METHODS

General Design

A total of 12 PET scans were acquired in 3 male baboons (*Papio anubis*, 25, 20 and 16

kg denoted A, B and C respectively), under 2 conditions (a non-carrier added [NCA] condition

followed by a carrier added condition [CA]), using 2 ligands ([^{11}C]raclopride and [^{11}C]NPA)

over a duration of 180 days. The difference between the first scan and the fourth scan was 91, 5

and 62 days for baboons A, B and C. The animals were not studied using any other radioligands

or pharmacological challenges during this period to avoid alterations in D$_2$ receptor status

The aim of this study was to determine the in vivo B_{max} and K_D for both [^{11}C]raclopride

and [^{11}C]NPA using the bolus plus constant infusion paradigm (BCI). This method has been

successfully used in the past to derive the B_{max} and K_D of tracers such as [^{123}I]iomazenil and

[^{123}I]IBF (Laruelle et al., 1994a; Laruelle et al., 1994b). Since plasma clearance obeys first-

order kinetics, there is a simple relationship between the injected mass of the radioligand and the concentrations at steady state. Assuming both [^{11}C]raclopride and [^{11}C]NPA cross the blood-brain barrier (BBB) by passive diffusion, the concentration of free radioligand is equal on both sides of the BBB at equilibrium, an assumption that has been empirically validated for other radiotracers (Laruelle et al., 1994a). Thus the BCI paradigm allows the relatively easy control of the concentration of free radioligand within the brain at steady state.

Preliminary experiments with both radiotracers were performed to define the optimal bolus-to-infusion ratio required to attain steady state for each animal. These experiments suggested that the bolus to infusion ratio (K_{bol}, the time that would be required to inject the bolus at the infusion rate) for [^{11}C]raclopride and [^{11}C]NPA should be 45-55 min and 50-65 min respectively.

To determine the optimal doses to use in CA experiments, K_D values of 1.2 nM and 0.15 nM were assumed for [^{11}C]raclopride and [^{11}C]NPA (Kohler et al., 1985; Narendran et al., 2004). The specific activity of the radioligand was controlled such that the targeted levels of receptor occupancy at steady-state would be less than 5% and about 60-70% for the NCA and CA experiments, respectively. For each animal, the sequence of radiotracers was counterbalanced to prevent bias in the between-radiotracer comparison.

Synthesis of [^{11}C]raclopride and [^{11}C]NPA

[^{11}C]Raclopride and [^{11}C]NPA were prepared as previously described. (Hwang et al., 2000; Mawlawi et al., 2001).

PET imaging protocol

Experiments were performed according to protocols approved by the Columbia University Medical Center Institutional Animal Care and Use Committee. Fasted animals were immobilized with ketamine (10 mg kg^{-1} i.m.) and anesthetized with 1.8% isoflurane via

endotracheal tube. Vital signs were monitored every 10 min and temperature was kept constant at 37°C with heated water blankets. An I.V. perfusion line was used for the injection of radiotracers and a catheter inserted in a femoral artery was used for arterial blood sampling.

PET imaging was performed with ECAT EXACT HR+ scanner (Siemens/CTI, Knoxville, TN). Following a 10-min transmission scan, emission data was collected in 3D mode for 90 min as successive frames (21 frames) of increasing duration for both [^{11}C]raclopride and [^{11}C]NPA.

Input function measurements

A total of 30 arterial samples were collected per experiment with an automated blood sampling system for the first four minutes followed by manual draws at various intervals. Following centrifugation (10 min at 1800g), plasma was collected and activity measured in 0.2 mL aliquots on a gamma counter (Wallac 1480 Wizard 3M Automatic Gamma Counter, Perkin-Elmer, Boston, MA).

For both [^{11}C]raclopride (2, 4, 16, 50, 60, and 80 min) and [^{11}C]NPA (1, 4, 12, 40, 60 and 80 min), six samples were further processed using previously described HPLC procedures (Mawlawi et al., 2001; Hwang et al., 2004) to measure the fraction of plasma activity representing unmetabolized parent compound. The parent fraction was calculated as the ratio of parent to total activity. The parent fractions were fitted to the sum of two exponentials. The smallest exponential of the fraction of the parent curve, λ_{par}, was constrained to the difference between λ_{cer} (the terminal rate of washout of the cerebellar activity) and λ_{tot} (the smallest elimination rate constant of the total plasma) (Abi-Dargham et al., 1999). The input function was then calculated as the product of the total counts and the interpolated fraction parent at each time point.

The measured input function values ($C_a(t)$, µCi mL^{-1}) were fitted to

$$C_a(t) = \sum_{i=1}^{2} C_{oi} e^{-\lambda_i t} + C_{ss} \sum_{i=1}^{2} f_{oi}(1 - e^{-\lambda_i t})$$ Eq. 3

where C_{0_i} is the zero time intercept of each exponential (nM), λ_1 is the elimination rate

constant (min-1) associated with each exponential, f_{0i} is the fraction of zero time intercept

associated with each exponential, and C_{SS} the free concentration at steady state (nM). The first

term of equation (Eq 3) represents activity due to the bolus and the second term the activity due

to the constant infusion. C_{SS} is related to clearance (C_L, L h-1) and the rate of infusion R_O (nmol

h-1), by

$$C_{SS} = \frac{R_0}{C_L}$$ Eq. 4

The plasma free fraction (f_1) was measured by ultrafiltration for both tracers using

techniques described previously (Narendran et al., 2004).

Image Analysis

The striatum and cerebellum ROIs (regions of interest) were delineated on each baboon's

brain MRI (a T1-weighted axial MRI sequence, acquired parallel to the anterior-posterior

commissure, TR 34 msec, TE 5 msec, flip angle of 45 degrees, slice thickness 1.5 mm, zero gap,

matrix 1.5 mm x 1 mm x 1mm voxels).

Attenuation-corrected PET emission data were reconstructed with filtered backprojection,

using a Shepp filter (cutoff 0.5 cycles/projection rays) and processed using the image analysis

software MEDx (Sensor Systems, Inc., Sterling, Virginia). An image was created by summing

all the frames, and this summed image was used to define the registration parameters for use

with the MRI, using the between-modality automated image registration (AIR) algorithm, as

described previously (Mawlawi et al., 2001). Registration parameters were then applied to the

individual frames for registration to the MRI data set. Regional boundaries were transferred to

the individual registered PET frames, and time-activity curves were measured. Right and left

striata were averaged. For a given animal, the same regional boundaries were used for both the

NCA and CA experiments.

Derivation of outcome measures

Distribution volumes

The regional tissue distribution volume (V_T, mL g^{-1}) was defined as the ratio of the

ligand concentration in a region (A_T, µCi mL^{-1}) to the concentration of unmetabolized ligand in

arterial plasma (C_{SS}, µCi mL^{-1}) at equilibrium

$$V_T = \frac{A_T}{C_{SS}}$$

Eq. 5

As the concentration of D$_2$ receptors is negligible in the cerebellum (Mawlawi et al.,

2001), only free and nonspecifically bound radiotracer were considered to contribute to V_T in the

cerebellum (V_T CER), and V_T CER was assumed to be equal to the nondisplaceable distribution

volume (V_2). The striatal V_T (V_T STR) included V_2 and the specific binding distribution volume

(V_3). It was assumed that the nondisplaceable distribution volume was equal in both regions.

Therefore, V_3 was derived as V_T STR minus V_T CER.

Binding parameters

The primary parameters of interest in this study were B_{max}, the concentration of sites

(nanomoles per L of tissue, nM), and K_D, the in vivo equilibrium dissociation constant of the

radiotracer (nanomoles per L of brain water, nM). Secondary parameters included the binding

potential (BP, ml g^{-1}) and the specific to nonspecific partition coefficient (V_3", unitless). BP and

V_3" are related to B_{max} and K_D by

$$BP = f_1 \frac{B_{max}}{K_D}$$

Eq. 6

$$V_3'' = f_2 \frac{B_{max}}{K_D} \qquad \text{Eq. 7}$$

where f_1 and f_2 are the free fractions in the plasma and the nondisplaceable compartment, respectively. BP and V_3'' were derived only in NCA experiments.

Derivation of B_{max} and K_D were determined by three analytical methods.

Method A. Simple equilibrium analysis

Equilibrium analysis was applied to the PET frames obtained from 40-90 minutes. The slope of the cerebellum and striatum activity over time expressed as a percentage of the mean value obtained from 40-90 minutes was used as a measure of the degree of equilibrium attained. The activity (μCi mL^{-1}) in the cerebellum (A_{CER}) and striatum (A_{STR}) were averaged from 40-90 minutes. $V_{T\ CER}$ was derived as

$$V_{T\ CER} = \frac{A_{CER}}{C_{SS}} \qquad \text{Eq. 8}$$

At equilibrium, the free tracer equilibrates across the blood-brain barrier so that the intracerebral free ligand concentration Fe (nM) is equal to the free ligand concentration in plasma

$$F_e = f_1 * C_{SS} = f_2 * A_{CER} \qquad \text{Eq. 9}$$

At equilibrium, the bound ligand concentration B_e (nM), was derived as

$$B_e = A_{STR} - A_{CER} \qquad \text{Eq. 10}$$

For each animal with each ligand, B_e and F_e data obtained from the NCA and CA experiments were fitted to the Scatchard plot equation (Scatchard, 1949)

$$\frac{B}{F} = \frac{-1}{K_D}(B - B_{max}) \qquad \text{Eq. 11}$$

with K_D and B_{max} determined by linear regression.

BP and V_3'' were derived in NCA experiments as $V_{T\ STR}$-$V_{T\ CER}$ and BP/$V_{T\ CER}$, respectively.

Method B. Kinetic Analysis

Analysis of NCA experiments. Kinetic estimations of [11C]raclopride and [11C]NPA V_T were performed using kinetic analysis and the arterial input function. [11C]Raclopride $V_{T\ CER}$ and $V_{T\ STR}$ were obtained using a one-tissue compartment model (1TCM, two kinetic parameters, K_1 and k_2). [11C]NPA $V_{T\ CER}$ and $V_{T\ STR}$ were obtained using a two-tissue compartments model (2TCM, four kinetic parameters, K_1 to k_4). The choice of 1TCM for [11C]raclopride and 2TCM for [11C]NPA was based on the goodness of fit.

In the 1TCM, V_T was derived from kinetic parameters as

$$V_T = \frac{K_1}{k_2} \qquad \text{Eq. 12}$$

In the 2TCM, V_T was derived from kinetic parameters as

$$V_T = \frac{K_1}{k_2}\left(1 + \frac{k_3}{k_4}\right) \qquad \text{Eq. 13}$$

Kinetic rate constants were estimated by nonlinear regression using a Levenberg-Marquardt least-squares minimization procedure implemented in MATLAB (Math Works). BP and V_3'' were derived as described above.

Analysis of CA experiments. Data were fitted to the following nonlinear system of differential equations (Sadzot et al., 1991; Slifstein et al., 2004a)

$$\frac{dC_2(t)}{dt} = K_1 Ca(t) - (k_2 + k_3)C_2(t) + k_+ C_2(t)C_3(t) + k_4 C_3(t) \qquad \text{Eq. 14}$$

$$\frac{dC_3}{dt} = k_3 C_2(t) - k_+ C_2(t)C_3(t) - k_4 C_3(t) \qquad \text{Eq. 15}$$

where C_a, C_2 and C_3 are the concentration in the arterial, nondisplaceable, and specific compartments, respectively and $k_+ = f_2 k_{on}$. K_D and B_{max} were determined as

$$K_D = f_2 \frac{k_4}{k_+} \qquad\qquad \text{Eq. 16}$$

$$B_{max} = \frac{k_3}{k_+} \qquad\qquad \text{Eq. 17}$$

All the parameters (other than f_2 which was derived as $f_2 = \dfrac{f_1}{V_{T\,CER}}$) were estimated by

nonlinear least squares regression of the data onto the numerical solution of the differential

equations with two constraints as previously described (Slifstein et al., 2004b): 1) the ratio K_1/k_2

in each experiment was constrained to $V_{T\,CER}$ as estimated in that experiment; 2) the total

regional distribution volume, $K_1/k_2 *(1+ k_3 /k_4)$, was constrained to the $V_{T\,STR}$ measured in

NCA experiments. All kinetic analysis was performed in the Matlab (Mathworks, Natuck MA)

software environment.

Method C. Modeled equilibrium analysis

The modeled equilibrium method was adapted from peak equilibrium analysis (Farde et

al., 1986) and modified as previously described (Slifstein et al., 2004b). Data from each

experiment were fitted by kinetic modeling as described above to yield modeled specifically

bound and free plus nonspecifically bound curves. B_e was determined as the peak of the

specifically bound curve. F_e was determined as f_2 times the value of the free plus nonspecifically

bound curve at the time of peak specific binding. In other words bound and free were both

estimated from the values of these parameters that were determined from the kinetic fit within

the region of interest itself and not from the difference between the region of interest and the

reference region. As the f_2 used in method C was obtained from the same kinetic fit outlined in

method B these methods were not truly independent of each other. For all 3 animals, data were

fitted to the Scatchard plot equation (Eq. 11) and K_D and B_{max} were determined as described

above.

Statistical analysis

Statistical analysis was performed with paired t tests to test differences between conditions (NCA and CA) unless otherwise specified. A two tailed probability value of $p \leq 0.05$ was selected as significant.

RESULTS

Injected dose and mass

The mean injected dose for [^{11}C]raclopride was 2.07 ± 0.56 mCi and 4.03 ± 1.45 mCi for the NCA (n=3) and CA (n=3) conditions, respectively. The mean injected mass for [^{11}C]raclopride was 1.05 ± 0.15 µg (3.0 ± 0.4 nmoles) and 336 ± 87 µg (969 ± 250 nmoles) for the NCA and CA conditions respectively.

The mean injected dose for [^{11}C]NPA was 2.96 ± 1.25 mCi and 3.60 ± 0.65 for the NCA (n=3) and CA (n=3) conditions respectively. The mean injected mass for [^{11}C]NPA was 1.24 ± 0.19 µg (4.2 ± 0.6 nmoles) and 180 ± 7 µg (611 ± 22 nmoles) for the NCA and CA conditions respectively.

Plasma parameters

Table 2 lists the plasma clearance, f_1, and C_{SS} for the NCA and CA conditions for both [^{11}C]raclopride and [^{11}C]NPA. Significant differences were evidenced in C_{SS} but not in clearance and f_1 between CA and NCA conditions for both tracers, demonstrating that the mass dose does not affect plasma clearance and nonspecific binding in plasma.

Brain activity

Figure 1 displays the MRI and coregistered PET [^{11}C]raclopride and [^{11}C]NPA images in NCA experiments in the same baboon. Both [^{11}C]raclopride (Figure 2) and [^{11}C]NPA (Figure 3) reached an acceptable equilibrium level (as defined above) by 40 min in both the striatum and

cerebellum. For [^{11}C]raclopride, changes over this interval were -2 ± 5%/h in the striatum and -8 ± 5%/h in the cerebellum. For [^{11}C]NPA, these changes were -1 ± 10%/h and -3 ± 10%/h in striatum and cerebellum.

Binding parameters

Method A. Simple equilibrium analysis

Table 2 lists V_2 and f_2 for the NCA and CA conditions for both [^{11}C]raclopride and [^{11}C]NPA. No significant differences were noted in V_2 and f_2 between CA and NCA conditions for both tracers, demonstrating that the mass dose does not affect cerebellum distribution volume for both tracers. Table 3 lists the F_e, B_e, BP and V_3'' for [^{11}C]raclopride and [^{11}C]NPA in all three baboons.

Table 4 lists the B_{max} and K_D of [^{11}C]raclopride and [^{11}C]NPA and the %R_{high} derived in all three baboons with the simple equilibrium analysis (see Figure 4).

Method B. Kinetic analysis

The mean kinetic V_2 for [^{11}C]raclopride was 0.91 ± 0.34 mL g^{-1} and 0.75 ± 0.27 mL g^{-1} for the NCA (n=3) and CA (n=3) conditions respectively (paired t test, $p = 0.15$). The mean kinetic BP and V_3'' was 2.53 ± 1.25 mL g^{-1} and 2.71 ± 0.36 for the [^{11}C]raclopride NCA condition.

The mean kinetic V_2 for [^{11}C]NPA was 6.30 ± 0.56 mL g^{-1} and 5.40 ± 1.03 mL g^{-1} for the NCA (n=3) and CA (n=3) conditions respectively (paired t test, $p = 0.38$). The mean kinetic BP and V_3'' was 6.08 ± 2.45 mL g^{-1} and 0.96 ± 0.33 for the [^{11}C]NPA NCA condition.

Table 4 lists the B_{max} and K_D of [^{11}C]raclopride and [^{11}C]NPA and the %R_{high} derived in all three baboons with the kinetic analysis. None of the outcome measures derived by kinetic analysis were significantly different from the outcome measures by simple equilibrium analysis.

Method C. Modeled equilibrium analysis

Table 4 lists the B_{max} and K_D of [11C]raclopride and [11C]NPA and the %R_{high} derived in all three baboons with the modeled equilibrium analysis. None of the outcome measures derived by the modeled equilibrium analysis were significantly different from the outcome measures derived by simple equilibrium and kinetic analysis.

DISCUSSION

The two main findings of this study are 1) the in vivo affinity of [11C]NPA is 0.16 nM and 2) the number of binding sites available to [11C]NPA at this affinity is 21.6 ± 2.8 nM, corresponding to 79% $\pm$ 2% of the sites available to [11C]raclopride (27.3 ± 3.9 nM). The technical strengths and weaknesses of the study design and the implications of these findings are discussed.

Agreement between the methods

In this study, K_D and B_{max} were derived using three methods. The simple equilibrium analysis requires the establishment of a sustained equilibrium state. As [11C]raclopride and [11C]NPA both have relatively fast kinetics, they achieved reasonable and comparable equilibria within the duration of the study. The agreement in the derivation of B_{max} and K_D between the kinetic analysis, which does not require attainment of equilibrium during the scan, and simple equilibrium analysis acted as an internal control. The agreement between these methods was strengthened by the modeled equilibrium analysis that integrates elements of each.

Opposite effects of raclopride and NPA on endogenous dopamine

The acute administration of D_2 antagonists and D_2 agonists at pharmacological doses during the CA condition induces an increase or decrease of dopamine concentration relative to that under tracer conditions (Bunney et al., 1973a; Bunney et al., 1973b). As this change in endogenous dopamine could present a source of potential artifact, the effect of such changes on

the measured in vivo B_{max} and K_D for the antagonist [11C]raclopride and agonist [11C]NPA as determined by a two-point Scatchard plot was assessed (see Appendix). This analysis shows that depending on the magnitude of change in endogenous dopamine concentrations following a pharmacological CA dose, both the B_{max} and K_D are underestimated for the antagonist [11C]raclopride and overestimated for the agonist [11C]NPA. The effect of this artifact would be to underestimate differences between [11C]raclopride and [11C]NPA maximal density of available sites (ie., %R_{high} might be lower, but not greater than the 79% estimated by our data).

Effects of anesthesia on fraction of R_{high}.

Another potential confound for this study is the effect of anesthesia (isoflurane and ketamine) on the binding parameters of both radiotracers. In vitro homogenate binding studies using anesthetic doses of ketamine and isoflurane have been shown to inhibit the high affinity state of D_2 receptors (Seeman and Kapur, 2003). It is possible that under unanesthetized conditions the in vivo [11C]NPA B_{max} and [11C]raclopride K_D may be higher than reported here due to a higher proportion of R_{high} and the resultant increased endogenous competition by dopamine. This is unlikely to change the [11C]raclopride B_{max} and [11C]NPA K_D. Future experiments in unanesthetized animals are necessary to address these issues.

[11C]Raclopride binding parameters

The in vivo K_D of [11C]raclopride measured in this study (1.59 ± 0.28 nM) was in agreement with in vitro values (see Table 5) reported to be in the 1 to 2 nM range. In contrast, the [11C]raclopride in vivo K_D reported in this study is lower than in vivo values reported using PET (Table 6), which range between 8 and 12 nM. As previously noted (Laruelle et al., 1994b) this discrepancy results from the use of total cerebellum activity to represent free ligand in the previous PET studies. Taking into account that only $14.6\% \pm 2.1\%$ of the cerebellum concentration is free (f_2, Table 2), the previously reported values of [11C]raclopride K_D would be

revised to approximately 1.5 nM after f_2 adjustment, consistent with the reported in vitro values as well as our in vivo [^{11}C]raclopride estimate of K_D.

This discrepancy in the definition of the free parameter does not affect the B_{max} estimate. The striatum [^{11}C]raclopride D_2 B_{max} (27.3 ± 3.9 nM) measured in this study is consistent with the range for striatum D_2 B_{max} reported in the PET literature (Table 6). Of note, two of the three animals used in this study were also included in a previous PET study measuring the B_{max} of another D_2 receptor antagonist of the benzamide family ([^{18}F]fallypride) (Slifstein et al., 2004b). The [^{18}F]fallypride B_{max} (28.0 ± 10.9 nM) measured in these two animals (baboon A & B) was very close to their [^{11}C]raclopride B_{max} measured here (27.0 ± 5.4 nM), highlighting the consistency of the B_{max} measurements with antagonist radioligands.

[^{11}C]NPA binding parameters

In vitro, the binding of NPA to D_2 receptors is best fitted by a two site model (Table 1), and the high affinity state is converted to low affinity state in the presence of GTP (Grigoriadis and Seeman, 1985). In this study, the two-point scatchard plots of [^{11}C]NPA fitted to a one-site model estimated an affinity of 0.16 ± 0.01 nM, values that are consistent with the affinity of NPA for D_2 $_{high}$ measured in vitro (Table 1). This agreement between the in vivo and in vitro values for K_D strongly suggest that the in vivo binding of [^{11}C]NPA measured with PET corresponds to binding to D_2 $_{high}$ receptors. In theory, an in vivo multiple point scatchard plot of [^{11}C]NPA could be fitted to a two site model. However, given the 70:30 ratio of $R_{high}:R_{low}$ (Narendran et al., 2004) and the likely 100 fold difference between the K_{high} and K_{low} (Sibley et al., 1982) this procedure would be problematic. This is because the inflection of the curve due to low affinity site binding would only become apparent at saturation levels greater than 80%, where the signal to noise ratio of PET is too low to provide useful data (see simulation in Figure

5). Therefore a 2-point fit was chosen based on the assumption that it would be representative of high affinity site binding.

The in vivo [^{11}C]NPA site density was significantly smaller than that of [^{11}C]raclopride, suggesting a difference in the nature of sites labeled by both compounds. Assuming this difference is because [^{11}C]NPA binds only to D$_{2\ high}$ and [^{11}C]raclopride binds to both D$_{2\ high}$ and D$_{2\ low}$, 79% $\pm$ 2% of D$_2$ receptors are D$_{2\ high}$. This also implies that, under tracer conditions, the contribution of D$_{2\ low}$ to [^{11}C]NPA BP is truly negligible. Using Eq. 1 and the results of the present study (%R$_{high}$ of 79%), the contribution of D2 low to [^{11}C]NPA BP would be only 0.26%.

The fundamental result of this study (R$_{high}$ = 79% $\pm$ 2%) is in agreement with the results of a previous study comparing the vulnerability of [^{11}C]raclopride and [^{11}C]NPA to endogenous competition by DA (Narendran et al., 2004). Three male baboons were studied with [^{11}C]raclopride and [^{11}C]NPA under baseline conditions and following administration of amphetamine. The amphetamine-induced decrease in binding potential (ΔBP) of [^{11}C]NPA was on average 1.42 times greater that of [^{11}C]raclopride at each dose tested. Assuming a 30% occupancy of D$_2$ receptors by DA in anesthetized baboons (Laruelle et al., 1997), the results of that study predicted the % R$_{high}$ to be 79% (see Figure 7 in Narendran et al., 2004), consistent with the direct measurement of % R$_{high}$ in the current study (79% $\pm$ 2%).

This result is also consistent with a recent PET study conducted in rhesus monkey by Kortekaas et al (2004). In that study the authors demonstrated the ability of another D$_2$/D$_3$ agonist (+)-PD 128907 (which in vitro demonstrates a relatively higher preference to bind to D$_3$ receptors) to displace striatal [^{11}C]raclopride binding in an orderly dose-dependent fashion that followed a one-site fit to a maximum of 85%. This led the authors to conclude that in vivo there was no evidence in favor of a multiple sight model representing the high and low affinity

receptors or the D_2 and D_3 subtype. Alternatively these results could be interpreted as evidence for a majority of D_2/D_3 receptors to be configured in a state of high affinity for agonists (Kortekaas et al., 2004).

The results of this study are also consistent with an in vitro study measuring $D_{2\,high}$ and $D_{2\,low}$ with autoradiography (Richfield et al., 1989), a setting in which endogenous receptor coupling is more likely to be preserved than in homogenates (where $\%R_{high}$ has been reported in the range of 12-50% (Sibley et al., 1982; Seeman et al., 2002)). Competition studies of [^{3}H]spiperone with dopamine revealed biphasic competition curves, and $\%R_{high}$ was 77%, a value in the range of our in vivo estimate (79%). Guanine nucleotides completely converted the high-affinity site to a low-affinity site. In contrast, for D_1 receptors, $\%R_{high}$ was only 21%. The difference in $\%R_{high}$ between D_1 and D_2 receptors might explain why the in vivo binding of D_2 and not D_1 receptor antagonist radioligands are decreased by challenges that increase endogenous DA (Abi-Dargham et al., 1999)

In conclusion, results of in vivo PET saturation experiments conducted in three baboons with the D_2 antagonist [^{11}C]raclopride and the D_2 agonist [^{11}C]NPA demonstrated a large proportion (70-80%) of D_2 receptors configured in $D_{2\,high}$ state in vivo. This is likely to contribute to the potency of endogenous DA to affect the binding of D_2 receptor radiotracers. This also indicates that at tracer dose, [^{11}C]NPA BP is almost exclusively associated with $D_{2\,high}$ sites. Thus [^{11}C]NPA appears to be an appropriate tool to study $D_{2\,high}$ in health and disease.

ACKNOWLEDGEMENT

REFERENCES

Abi-Dargham A, Simpson N, Kegeles L, Parsey R, Hwang DR, Anjilvel S, Zea-Ponce Y, Lombardo I, Van Heertum R, Mann JJ, Foged C, Halldin C and Laruelle M (1999) PET studies of binding competition between endogenous dopamine and the D1 radiotracer [11C]NNC 756. *Synapse* **32**:93-109.

Alberts GL, Pregenzer JF and Im WB (2000) Advantages of heterologous expression of human D2long dopamine receptors in human neuroblastoma SH-SY5Y over human embryonic kidney 293 cells. *Br J Pharmacol* **131**:514-520.

Bunney BS, Aghajanian GK and Roth RH (1973a) Comparison of effects of L-dopa, amphetamine and apomorphine on firing rate of rat dopaminergic neurones. *Nat New Biol* **245**:123-125.

Bunney BS, Walters JR, Roth RH and Aghajanian GK (1973b) Dopaminergic neurons: effect of antipsychotic drugs and amphetamine on single cell activity. *J Pharmacol Exp Ther* **185**:560-571.

Carson RE, Channing MA, Der MG, Herscovitch P and Eckelman W (2002) Scatchard analysis with bolus/infusion administration of [11C]raclopride: amphetamine effects in anesthetized monkeys, in *Brain Imaging Using PET* (Senda M, Kimura Y and Herscovitch P eds) pp 63-69, Academic Press, San Diego.

Doudet DJ, Jivan S, Ruth TJ and Holden JE (2002) Density and affinity of the dopamine D2 receptors in aged symptomatic and asymptomatic MPTP-treated monkeys: PET studies with [11C]raclopride. *Synapse* **44**:198-202.

Farde L, Hall H, Ehrin E and Sedvall G (1986) Quantitative analysis of D2 dopamine receptor binding in the living human brain by PET. *Science* **231**:258-261.

Farde L, Hall H, Pauli S and Halldin C (1995) Variability in D2-dopamine receptor density and affinity: a PET study with [11C]raclopride in man. *Synapse* **20**:200-208.

Gardner B and Strange PG (1998) Agonist action at D2(long) dopamine receptors: ligand binding and functional assays. *Br J Pharmacol* **124**:978-984.

George SR, Watanabe M and Seeman P (1985) Dopamine D2 receptors in the anterior pituitary: a single population without reciprocal antagonist/agonist states. *J Neurochem* **44**:1168-1177.

Ginovart N, Farde L, Halldin C and Swahn CG (1997) Effect of reserpine-induced depletion of synaptic dopamine on [C-11]raclopride binding to D-2-dopamine receptors in the monkey brain. *Synapse* **25**:321-325.

Grigoriadis D and Seeman P (1985) Complete conversion of brain D2 dopamine receptors from the high- to the low-affinity state for dopamine agonists, using sodium ions and guanine nucleotide. *J Neurochem* **44**:1925-1935.

Hall H, Halldin C and Sedvall G (1992) Gpp(NH)p stimulates [3H]raclopride binding to homogenates from human putamen and accumbens. *Neurosci Lett* **136**:79-82.

Hall H, Wedel I and Sallemark M (1988) Effects of temperature on the in vitro binding of 3H-raclopride to rat striatal dopamine-D2 receptors. *Pharmacol Toxicol* **63**:118-121.

Hietala J, Nagren K, Lehikoinen P, Ruotsalainen U and Syvalahti E (1999) Measurement of striatal D2 dopamine receptor density and affinity with [11C]-raclopride in vivo: a test-retest analysis. *J Cereb Blood Flow Metab* **19**:210-217.

Holden JE, Jivan S, Ruth TJ and Doudet DJ (2002) In vivo receptor assay with multiple ligand concentrations: an equilibrium approach. *J Cereb Blood Flow Metab* **22**:1132-1141.

Hwang D, Kegeles LS and Laruelle M (2000) (-)-N-[(11)C]propyl-norapomorphine: a positron-labeled dopamine agonist for PET imaging of D(2) receptors. *Nucl Med Biol* **27**:533-539.

Hwang DR, Narendran R, Huang Y, Slifstein M, Talbot PS, Sudo Y, Van Berckel BN, Kegeles LS, Martinez D and Laruelle M (2004) Quantitative Analysis of (-)-N-(11)C-Propyl-Norapomorphine In Vivo Binding in Nonhuman Primates. *J Nucl Med* **45**:338-346.

Kohler C, Hall H, Ogren SO and Gawell L (1985) Specific in vitro and in vivo binding of 3H-raclopride. A potent substituted benzamide drug with high affinity for dopamine D-2 receptors in the rat brain. *Biochemical Pharmacology* **34**:2251-2259.

Kortekaas R, Maguire RP, Cremers TI, Dijkstra D, van Waarde A and Leenders KL (2004) In vivo binding behavior of dopamine receptor agonist (+)-PD 128907 and implications for the "ceiling effect" in endogenous competition studies with [(11)C]raclopride-a positron emission tomography study in Macaca mulatta. *J Cereb Blood Flow Metab* **24**:531-535.

Lahti RA, Mutin A, Cochrane EV, Tepper PG, Dijkstra D, Wikstrom H and Tamminga CA (1996) Affinities and intrinsic activities of dopamine receptor agonists for the hD21 and hD4.4 receptors. *Eur J Pharmacol* **301**:R11-13.

Laruelle M, Abi-Dargham A, Al-Tikriti MS, Baldwin RM, Zea-Ponce Y, Zoghbi SS, Charney DS, Hoffer PB and Innis RB (1994a) SPECT quantification of [123I]iomazenil binding to benzodiazepine receptors in nonhuman primates. II. Equilibrium analysis of constant infusion experiments and correlation with in vitro parameters. *J. Cereb. Blood Flow Metab.* **14**:453-465.

Laruelle M, Al-Tikriti MS, Zea-Ponce Y, Zoghbi SS, Baldwin RM, Charney DS, Hoffer PB, Kung HF and Innis RB (1994b) In vivo quantification of dopamine D2 receptors parameters in nonhuman primates with [^{123}I]iodobenzofuran and single photon emission computerized tomography. *Eur. J. Pharmacol.* **263**:39-51.

Laruelle M, Iyer RN, Al-Tikriti MS, Zea-Ponce Y, Malison R, Zoghbi SS, Baldwin RM, Kung HF, Charney DS, Hoffer PB, Innis RB and Bradberry CW (1997) Microdialysis and SPECT measurements of amphetamine-induced dopamine release in nonhuman primates. *Synapse* **25**:1-14.

Mawlawi O, Martinez D, Slifstein M, Broft A, Chatterjee R, Hwang DR, Huang Y, Simpson N, Ngo K, Van Heertum R and Laruelle M (2001) Imaging human mesolimbic dopamine

transmission with positron emission tomography: I. Accuracy and precision of D2

receptor parameter measurements in ventral striatum. *J Cereb Blood Flow Metab*

21:1034-1057.

Narendran R, Hwang DR, Slifstein M, Talbot PS, Erritzoe D, Huang Y, Cooper TB, Martinez D,

Kegeles LS, Abi-Dargham A and Laruelle M (2004) In vivo vulnerability to competition

by endogenous dopamine: Comparison of the D2 receptor agonist radiotracer (-)-N-

[11C]propyl-norapomorphine ([11C]NPA) with the D2 receptor antagonist radiotracer

[11C]-raclopride. *Synapse* **52**:188-208.

Neumeyer JL, Neustadt BR, Oh KH, Weinhardt KK, Boyce CB, Rosenberg FJ and Teiger DG

(1973) Aporphines. 8. Total synthesis and pharmacological evaluation of (plus or minus)-

apomorphine, (plus or minus)-apocodeine, (plus or minus)-N-n- propylnorapomorphine,

and (plus or minus)-N-n-propylnorapocodeine. *J Med Chem* **16**:1223-1228.

Richfield EK, Penney JB and Young AB (1989) Anatomical and affinity state comparisons

between dopamine D1 and D2 receptors in the rat central nervous system. *Neuroscience*

30:767-777.

Roberts DJ and Strange PG (2005) Mechanisms of inverse agonist action at D2 dopamine

receptors. *Br J Pharmacol* **145**:34-42.

Sadzot B, Price JC, Mayberg HS, Douglass KH, Dannals RF, Lever JR, Ravert HT, Wilson AA,

Wagner HN, Jr., Feldman MA and Frost JJ (1991) Quantification of human opiate

receptor concentration and affinity using high and low specific activity

[¹¹C]diprenorphine and positron emission tomography. *J. Cereb. Blood Flow Metab.*

11:204-219.

Scatchard G (1949) The attraction of proteins for small molecules and ions. *Ann NY Acad Sci*

51:660-672.

Seeman P (2002) Atypical antipsychotics: mechanism of action. *Can J Psychiatry* **47**:27-38.

Seeman P and Kapur S (2003) Anesthetics inhibit high-affinity states of dopamine D2 and other

    G-linked receptors. *Synapse* **50**:35-40.

Seeman P, Niznik HB, Guan HC, Booth G and Ulpian C (1989) Link between D1 and D2

    dopamine receptors is reduced in schizophrenia and Huntington diseased brain. *Proc Natl*

    Acad Sci U S A **86**:10156-10160.

Seeman P, Tallerico T, Ko F, Tenn C and Kapur S (2002) Amphetamine-sensitized animals

    show a marked increase in dopamine D2 high receptors occupied by endogenous

    dopamine, even in the absence of acute challenges. *Synapse* **46**:235-239.

Seeman P and Van Tol HH (1994) Dopamine receptor pharmacology. *Trends Pharmacol Sci*

    15:264-270.

Seeman P, Watanabe M, Grigoriadis D, Tedesco JL, George SR, Svensson U, Nilsson JL and

    Neumeyer JL (1985) Dopamine D2 receptor binding sites for agonists. A tetrahedral

    model. *Mol Pharmacol* **28**:391-399.

Sibley DR, De Lean A and Creese I (1982) Anterior pituitary receptors: Demonstration of

    interconvertible high and low affinity states of the D_2 dopamine receptor. *J. Biol. Chem.*

    257:6351-6361.

Slifstein M, Hwang DR, Huang Y, Guo N, Sudo Y, Narendran R, Talbot P and Laruelle M

    (2004a) In vivo affinity of [18F]fallypride for striatal and extrastriatal dopamine D2

    receptors in nonhuman primates. *Psychopharmacology (Berl)* **175**:274-286.

Slifstein M, Hwang DR, Huang Y, Guo NN, Sudo Y, Narendran R, Talbot P and Laruelle M

    (2004b) In vivo affinity of [18F]fallypride for striatal and extrastriatal dopamine D2

    receptors in nonhuman primates. *Psychopharmacology* **In press**.

FOOTNOTES

a. Unnumbered Footnote

FIGURE LEGENDS

Figure 1. MRI and coregistered PET images of the NCA experiments for [^{11}C]raclopride and [^{11}C]NPA in the same baboon (time activity curves in the brain and plasma for these NCA experiments are represented in Figure 2 and Figure 3). The PET images represent the mean activity from 40-90 minutes (equilibrium frames) for both radiotracers. For comparison, the injected doses of both tracers were normalized.

Figure 2 Upper Panel: [^{11}C]raclopride concentration in cerebellum (closed circles) and striatum (closed squares) following bolus plus constant infusion (K$_{bol}$ 45 min) of NCA (upper left panel; injected mass of [^{11}C]raclopride 2.60 nmoles) and CA conditions (upper right panel; injected mass of [^{11}C]raclopride 1197 nmoles) in baboon A. Lower Panel: Corresponding arterial total activity (open circles) and [^{11}C]raclopride parent concentration (closed circles) for the NCA (lower left panel) and CA (lower right panel) conditions shown above. Also shown in the figure are the measured values fitted to Eq. 3 (solid line) to calculate clearance and C$_{SS}$.

Figure 3. Upper Panel: [^{11}C]NPA concentration in cerebellum (closed circles) and striatum (closed squares) following bolus plus constant infusion (K$_{bol}$ 55 min) of NCA (upper left panel; injected mass of [^{11}C]NPA 3.66 nmoles) and CA conditions (upper right panel; injected mass of [^{11}C]NPA 602 nmoles) in baboon A. Lower Panel: Corresponding arterial total activity (open circles) and [^{11}C]NPA parent concentration (closed circles) for the NCA (lower left panel) and CA (lower right panel) conditions shown above. Also shown in the figure are the measured values fitted to Eq. 3 (solid line) to calculate clearance and C$_{SS}$.

Figure 4. Scatchard analysis of saturation data derived using equilibrium analysis for [^{11}C]raclopride (open circles) and [^{11}C]NPA (closed squares) in three baboons. Note the B_{max} of [^{11}C]raclopride is greater than the B_{max} of [^{11}C]NPA in all three animals. In Figure B/F in Y-axis represents Bound/Free.

Figure 5. Simulated Scatchard plot resulting from multiple concentrations experiments using the following parameters: $R_{high} = 79$; $R_{low} = 12$; $K_{high} = 0.16$ nM; $K_{low} = 26$ nM. The figure shows the B/F (Bound/Free) versus Bound regression lines corresponding to [^{11}C]NPA binding to $D_{2\ high}$ (closed circles), $D_{2\ low}$ (closed squares) and total D_2 receptors (open circles). The presence of $D_{2\ low}$ is only manifested by a small inflexion in the regression line close to the full saturation level. Thus, even with such a large number of points, direct measurement of K_{low} and R_{low} is not feasible in vivo.

Table 1. In vitro affinity of NPA for $D_{2\,high}$ and $D_{2\,low}$ as reported in the literature.

Reference	D_2 Source	Ki $D_{2\,high}$ (nM)	Ki $D_{2\,low}$ (nM)	$D_{2\,high}$ /$D_{2\,low}$ selectivity
(Sibley et al., 1982)	Bovine anterior pituitary membranes	0.27	26	96
(Seeman et al., 1985)	Rat striatal membrane	0.40	23	58
(George et al., 1985)	Porcine anterior pituitary membranes	0.31	207	664
(Lahti et al., 1996)	CHO cells expressing human D2 (long)	0.07	14	208
(Gardner and Strange, 1998)	CHO cells expressing human D2 (long)	0.38	16	42

Table 2. Plasma and non specific binding parameters for simple equilibrium analysis.

Parameter	[^{11}C]Raclopride			[^{11}C]NPA		
	NCA (n=3)	CA (n=3)	p	NCA (n=3)	CA (n=3)	p
Clearance (L h^{-1})	16.27 ± 2.11	16.30 ± 5.21	0.99	52.44 ± 5.21	43.64 ± 10.41	0.27
f_1 (unitless)	13.1% ± 3.0%	11.7% ± 2.6%	0.36	6.0% ± 1.6%	6.1% ± 1.6%	0.18
C_{SS} (nM)	0.08 ± 0.01	26.81 ± 10.30	0.05	0.03 ± 0.01	5.93 ± 1.26	0.01
V_2 (mL g^{-1})	0.89 ± 0.21	0.83 ± 0.28	0.30	6.41 ± 0.78	5.83 ± 0.48	0.15
f_2 (unitless)	14.6% ± 2.1%	14.6% ± 2.1%	0.92	0.9% ± 0.2%	1.1% ± 0.3%	0.12

NCA: non carrier added; CA: carrier added; Clearance: plasma clearance of the parent compound; f_1: free fraction of the radiotracer in plasma; C_{SS}: parent compound concentration at steady state. V_2: distribution volume of the cerebellum relative to total plasma parent concentration; f_2: free fraction in the cerebellum.

Table 3. Binding Parameters derived from the simple equilibrium analysis.

| Baboon | Condition | $[^{11}C]$raclopride | | | | $[^{11}C]$NPA | | | |
| | | F_e | B_e | BP | V_3'' | F_e | B_e | BP | V_3'' |
		(nM)	(nM)	(mL g-1)	(unitless)	(nM)	(nM)	(mLg-1)	(unitless)
A	NCA	0.0108	0.232	3.35	3.00	0.0021	0.275	9.93	1.37
	CA	3.65	22.2	0.89	0.78	0.340	15.9	3.55	0.57
B	NCA	0.0086	0.137	1.55	2.25	0.0018	0.221	7.82	1.37
	CA	1.79	12.9	0.73	1.21	0.427	13.8	2.07	0.39
C	NCA	0.0109	0.159	2.02	2.35	0.0016	0.208	5.64	0.90
	CA	3.91	18.8	0.50	0.67	0.294	14.1	2.12	0.35

NCA: non carrier added; CA: carrier added; F_e: equilibrium intracerebral free ligand concentration; B_e: equilibrium bound ligand

concentration; BP: binding potential ($f_1 B_{max}/K_D$); V_3'': specific to nonspecific equilibrium partition coefficients ($f_2 B_{max}/K_D$).

Table 4. Derivation of B_{max} and K_D for [11C]raclopride and [11C]NPA using all three methods.

Method	Baboon	[11C]raclopride		[11C]NPA		Rhigh (%)
		K_D (nM)	B_{max} (nM)	K_D (nM)	B_{max} (nM)	
Simple Equilibrium Analysis (method A)	A	1.42	30.83	0.18	24.26	79%
	B	1.44	23.12	0.15	18.67	81%
	C	1.91	28.04	0.16	21.86	78%
	Mean + SD	1.59 ± 0.28	27.3 ± 3.9	0.16 ± 0.01	21.6 ± 2.80	79% ± 2%
Kinetic Analysis (method B)	A	1.52	30.67	0.23	22.20	72%
	B	2.11	21.48	0.20	17.76	83%
	C	1.48	27.78	0.17	21.29	77%
	Mean + SD	1.70 ± 0.35	26.6 ± 4.7	0.20 ± 0.03	20.4 ± 2.34	77% ± 5%
Modeled Equilibrium Analysis (method C)	A	1.22	28.70	0.11	21.61	75%
	B	2.54	22.96	0.16	17.06	74%
	C	2.12	29.05	0.20	22.95	79%
	Mean + SD	1.88 ± 0.93	26.9 ± 3.4	0.16 ± 0.05	20.5 ± 3.09	76% ± 2%

Table 5. In vitro affinity of raclopride for D_2 receptors.

| Reference	D_2 Source	K_D (nM)
(Kohler et al., 1985)	Rat striatal membrane	1.2
(Hall et al., 1988)	Rat striatal membrane (15 –37 degrees)	1.6-3.0
(Seeman et al., 1989)	Human striatal membrane	1.9
(Hall et al., 1992)	Human putamen membrane	1.0
(Hall et al., 1992)	Human accumbens membrane	1.1
(Seeman, 2002)	Human D2 long CHO cells membrane	1.7
(Alberts et al., 2000)	Human D2 long SH-SY5Y cells membrane	1.4
(Alberts et al., 2000)	Human D2 long HEK293 cells membrane	1.1

Table 6. In vivo striatal K_D and B_{max} of [^{11}C]raclopride in human and nonhuman primates

Reference	Species	Free parameter	K_D (nM)	Bmax (nM)
(Holden et al., 2002)	Rhesus	NSB	12 ±1	22 ±1
(Doudet et al., 2002)	Rhesus	NSB	11 ±1	21 ±2
(Carson et al., 2002)	Rhesus	NSB	12±2	35±6
(Ginovart et al., 1997)	Cynomolgus	NSB	9 ±1	34 ±2
This study	Baboon	Free	1.59 ± 0.3	27 ± 4
(Farde et al., 1995)	Human	NSB	9 ±2	28 ±7
(Hietala et al., 1999)	Human	NSB	8 ±0	24 ±4

Page 36
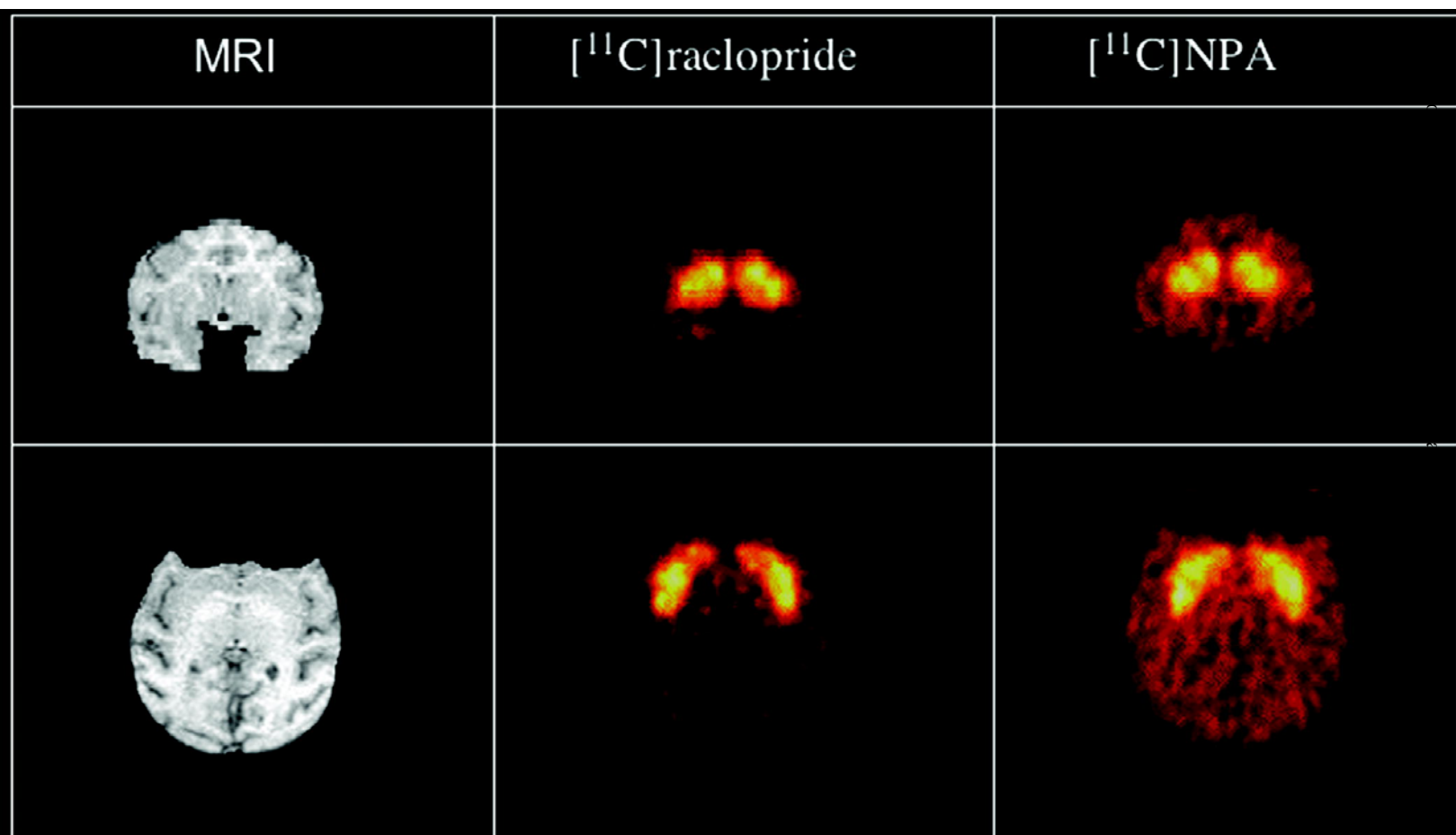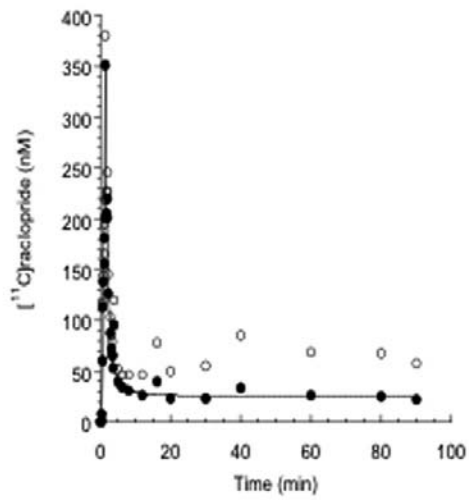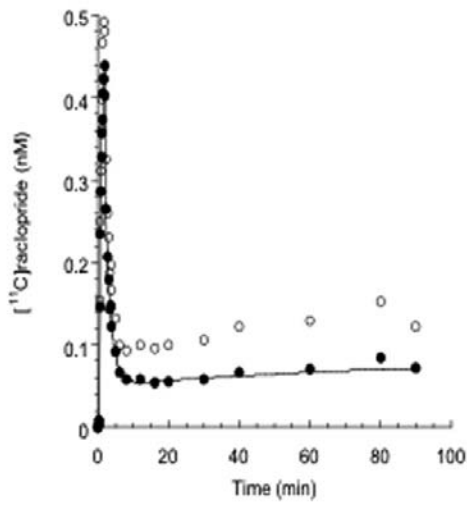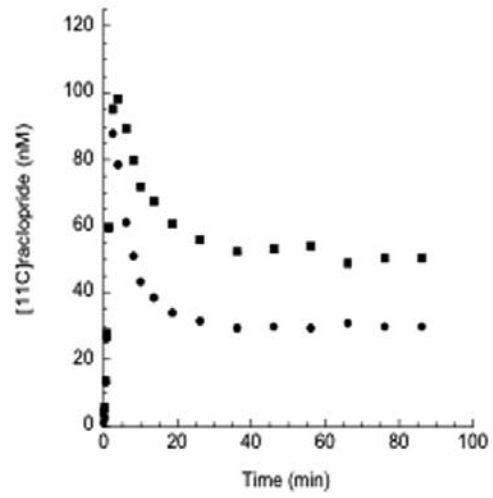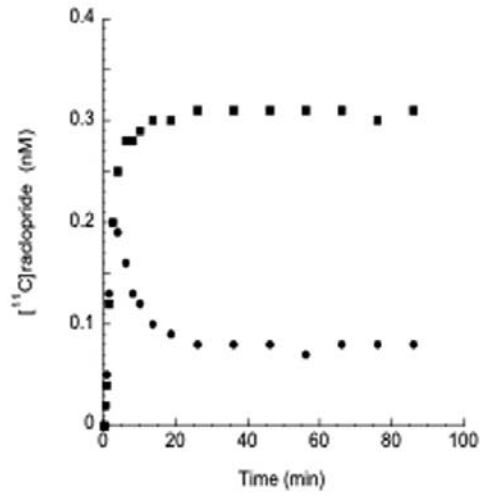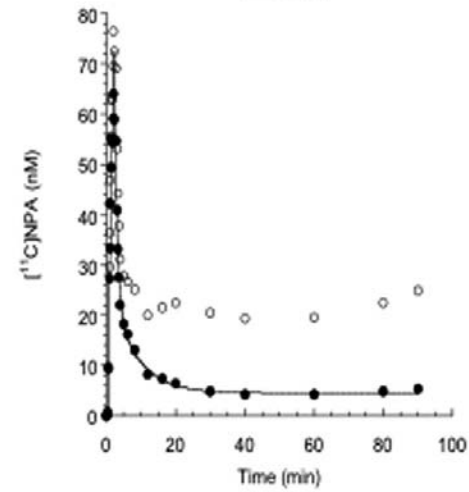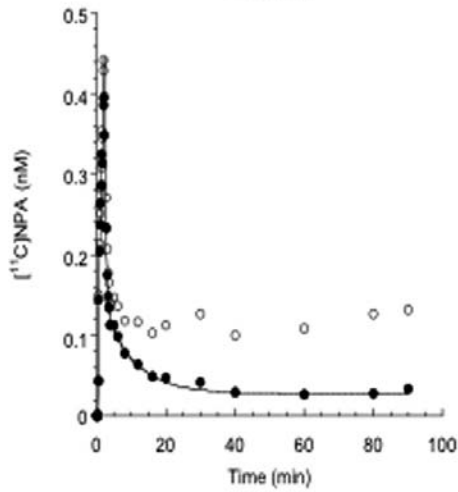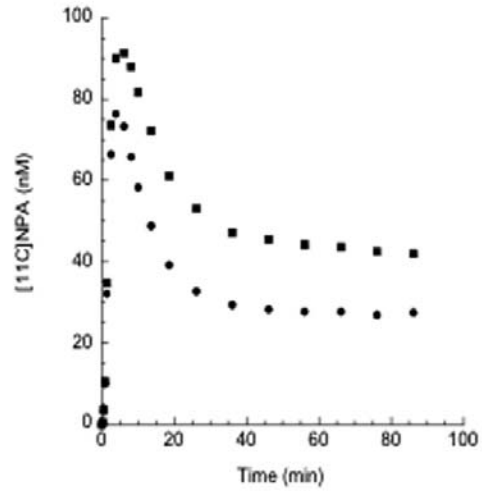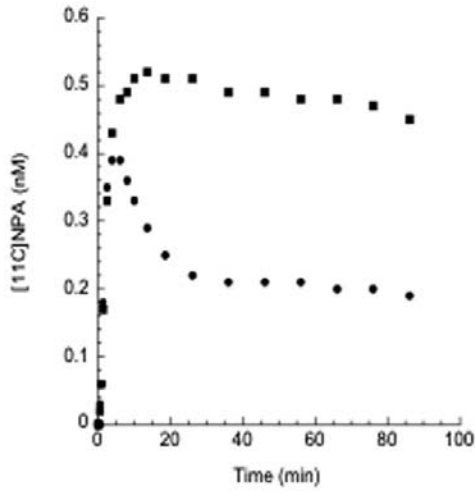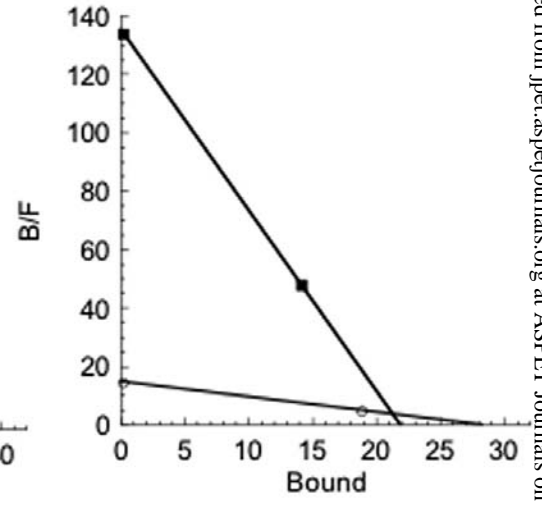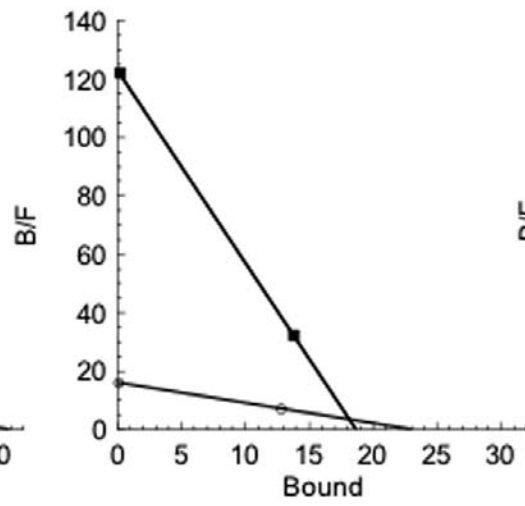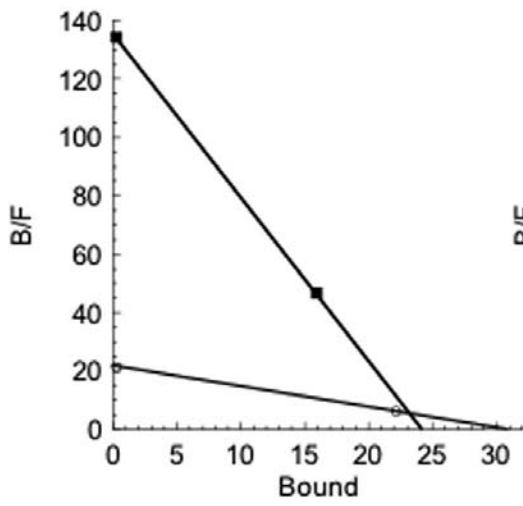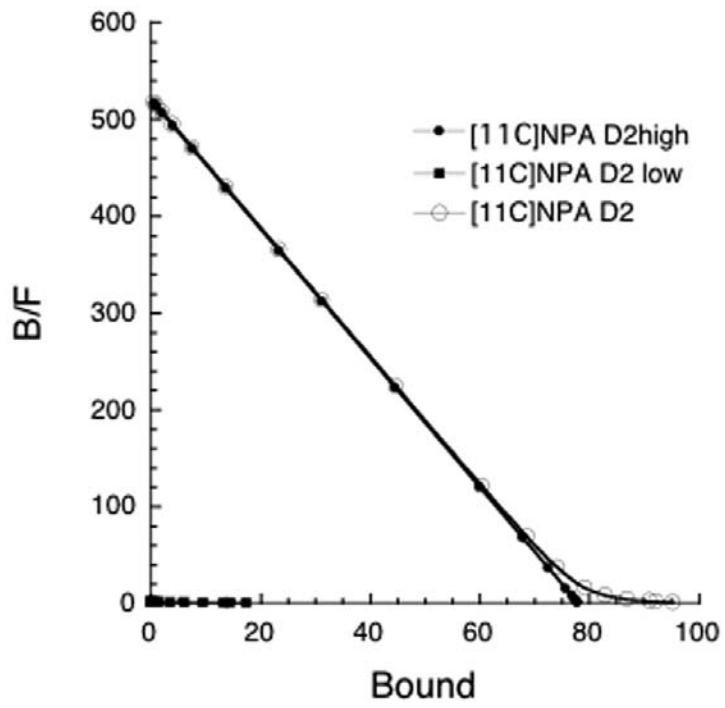
APPENDIX

1. Effect of pharmacological dose of antagonist versus agonist on in vivo affinity as determined by Scatchard plot.

We examine the effect on K_D determined by 2 point Scatchard plot when the high occupancy dose has pharmacological effects. We look at 2 cases – increased extracellular endogenous neurotransmitter during the high mass dose (antagonist) and decreased endogenous neurotransmitter (agonist) during the high mass dose. In each case we assume that there is baseline occupancy by endogenous transmitter, so that the reference value is not K_D, but $K_D' = K_D(1 + R)$ where R is the baseline ratio of the extracellular concentration of endogenous ligand to its inhibition constant.

Case 1: Antagonist

In this case the equilibrium equations for the low mass and high mass doses are

$$B_L = B_{max} \frac{F_L}{K_D' + F_L} \quad (low\ mass) \qquad \text{Eq A 1}$$

$$B_H = B_{max} \frac{F_H}{K_D'(1+\gamma) + F_H} \quad (high\ mass) \qquad \text{Eq A 2}$$

where B_L, F_L, B_H and F_H are bound and free radiotracer under low and high mass dose conditions, K_D' is as described above, and $\gamma = R_2/(1+R_1)$ where R_2 is the increase in the ratio R following the high mass dose.

By dividing these expressions by F to obtain B/F and rearranging to obtain the slope $(B_H/F_H - B_L/F_L)/(B_H-B_L)$, the measured Scatchard slope $-1/\hat{K}_D$ is seen to equal

$$\frac{-1}{\hat{K}_D} = \frac{-1}{K_D'} \left(\frac{1 + \gamma \dfrac{B_{max} - B_L}{B_H - B_L}}{1 + \gamma} \right) = \frac{-1}{K_D'} f \qquad \text{Eq A 3}$$

where the factor f is the expression in parentheses.

A 1

From this it follows that K_D' is f times as large as $\hat{K}_D$. Note first, that f always exceeds 1 because the expression $(B_{max}-B_L)/(B_H-B_L)$ always exceeds 1. Because, lacking evidence to the contrary, the endogenous neurotransmitter level during the high mass measurement is potentially orders of magnitude larger than the baseline level, the range of the term γ is effectively unbounded. As γ becomes infinitely large, f approaches $(B_{max} - B_L)/(B_H - B_L)$. Making the realistic assumption that $B_L << B_H < B_{max}$, the limiting value of f is approximately B_{max}/B_H. In other words, K_D' exceeds $\hat{K}_D$ at most by the reciprocal of the radioligand occupancy of the high mass scan. If, for example, during the high mass measurement there is 70% occupancy by radioligand, then the bounds on K_D' are $\hat{K}_D \leq K_D' \leq 1.43\hat{K}_D$.

Case 2: Agonist

For clarity we make the simplifying assumption that, following the high mass dose, the extracellular concentration of endogenous neurotransmitter is 0. In this case, the conditions are

$$B_L = B_{max} \frac{F_L}{K_D' + F_L} \quad (low\ mass) \qquad \text{Eq A 4}$$

$$B_H = B_{max} \frac{F_H}{K_D + F_H} \quad (high\ mass) \qquad \text{Eq A 5}$$

where the K_D appearing in the denominator of the high mass expression is the true in vivo K_D, not K_D'.

For this case, the Scatchard slope is

$$\frac{-1}{\hat{K}_D} = \frac{-1}{K_D'}\left(1 - R\frac{B_{max} - B_H}{B_H - B_L}\right) = \frac{-1}{K_D'}\left(1 - \frac{occ_{EN}}{1 - occ_{EN}} * \frac{B_{max} - B_H}{B_H - B_L}\right) \qquad \text{Eq A 6}$$

The term occ_{EN} is the baseline occupancy by endogenous neurotransmitter. Making the same assumption as above that $B_L << B_H$ and defining occ_{RL} as the occupancy by radioligand during the high mass measurement, this becomes

A 2

$$K_D' = \hat{K}_D\left(1 - \frac{occ_{EN}}{1-occ_{EN}} * \frac{1-occ_{RL}}{occ_{RL}}\right) \qquad \text{Eq A 7}$$

With the further assumption as above that $B_H = 0.7\ B_{max}$, this reduces to

$$K_D' = \hat{K}_D\left(1 - \frac{3}{7} * \frac{occ_{EN}}{1-occ_{EN}}\right) \qquad \text{Eq A 8}$$

For occ_{EN} in the literature range of 10 to 30%, the bounds on KD' are $0.82\,\hat{K}_D \leq K_D' \leq 0.95\ \hat{K}_D$.

2. Effect of pharmacological dose of antagonist versus agonist on in vivo B_{max} as determined by Scatchard plot.

Rearrangement of the Scatchard equation to isolate the B_{max} estimator leads to

$$\begin{aligned}
\hat{B}_{max} &= \frac{B}{F}\hat{K}_D + B \\
&= \frac{B}{F}\frac{K_D'}{f} + B
\end{aligned} \qquad \text{Eq A 9}$$

where f refers to the factor by which KD' is changed, as described in the 2 cases above. For the present case, where there are 2 points (high and low mass), both points are on the regression line, so these equations are an identity; either the low or high mass observed values can be substituted into the equation and equality will be preserved.

When the low mass values are substituted into the equation, the formula is the same for both the agonist and antagonist cases, although the meaning of the factor f is different in the two cases, as above. The result is

$$\hat{B}_{max} = B_{max}\left(\frac{K_D'/f + F_L}{K_D' + F_L}\right) \qquad \text{Eq A 10}$$

Making the same tracer dose approximation as above, such that $F_L \ll$ KD', this is approximately

$$\frac{B_{max}}{f} \qquad \text{Eq A 11}$$

A 3

i.e. the Bmax estimate will be altered in the same direction and to approximately the same extent as the affinity estimate. This result has the intuitive interpretation that if the low mass scan is performed under truly tracer dose conditions, then the datum (B_L, B_L /F_L) will be very close to the y axis, so that rotations of a line about this point will cause little change in the y axis intercept, i.e. true binding potential (B_{max}/K_D without reference to any free fraction) will be nearly preserved. Since the ratio of the two factors remains relatively unchanged, the factors themselves will be altered to the same extent.